ORIGINAL ARTICLE

Roel Neggers · Bjorn Stevens · J. David Neelin

A simple equilibrium model for shallow-cumulus-topped mixed layers

Abstract A new equilibrium model for shallow-cumulus-topped mixed layers is presented. A variant on the w_* closure for the shallow-cumulus mass flux is applied that retains the convective area-fraction in its formulation. As opposed to being constant, the fraction is explicitly modeled using a statistical closure as a function of the saturation deficit and humidity variance at cloud base. As a consequence, important new interactions are introduced between the convective transport, humidity, and depth of the mixed layer. This mechanism, which we call the mass-flux humidity feedback, helps determine the character of the equilibrium state such that the mixed-layer top is maintained close to the cloud-base height. Due to the strong sensitivity of the mass flux to the area fraction, the latter thus acts as a regulator or valve mechanism on moist convective transport. As a consequence, the mixed-layer model is able to explain the robustness of many aspects of the shallow-cumulus boundary layer that is typically found in observations and large-eddy simulations (LESs). The model is evaluated for a single-LES case as well as for global climatology obtained from a 40-year reanalysis of meteorological data by the European Centre for Medium-range Weather Forecasts (ECMWF). LES characteristics of convective mass flux, cloud fraction, humidity variance, cloud-base height, and surface fluxes of heat and humidity are reproduced. The solution on reanalysis fields reproduces the spatial structure of mixed-layer temperature and humidity and their associated surface fluxes in the subtropical Atlantic and Pacific trade wind regions. Furthermore, the spatial structure of the convective area-fraction matches that of synoptic surface observations of frequency of occurrence of shallow cumulus. Particularly striking is the smooth onset of the convective area-fraction and mass flux along the trade-wind trajectory that is reproduced, from zero to typical trade-wind values. The cumulus onset represents the necessity for shallow-cumulus mass flux to occur in order to close the mixed-layer budgets of heat, moisture, and mass, as a response to the changing magnitude of large-scale subsidence and free tropospheric humidity along the trajectory. Finally, the mass flux model is implemented in an intermediate-complexity tropical climate model to study its behavior when fully interactive with the larger-scale flow. A climate run then shows that the model is stable, due to the mass-flux humidity feedback acting to keep the shallow-cumulus boundary layer close to its equilibrium state for long, climatological timescales.

Communicated by R. Klein.

R. Neggers · B. Stevens · J. D. Neelin
Department of Atmospheric and Oceanic Sciences, University of California at Los Angeles (UCLA),
Los Angeles, CA, USA

Present address:
R. Neggers (✉)
European Centre for Medium-range Weather Forecasts (ECMWF), Shinfield Park,
Reading, Berkshire RG2 9AX, UK
E-mail: Roel.Neggers@ecmwf.int

1 Introduction

The budgets of heat and humidity in the steady-state marine shallow cumulus boundary layer result from a delicate balance among surface heat and moisture fluxes, dry and moist convective transport, radiation, and transport by the large-scale flow [28,31,40]. The exact state of the associated shallow-cumulus cloud population is an expression of this balance. For example, moist convective mass flux dominates vertical transport, strongly affecting the thermodynamic state of the boundary layer. Yet cloud occurrence necessary for moist convection in turn strongly depends on humidity conditions. As a consequence, explaining cloud occurrence requires a proper understanding of the interactions and feedbacks between all processes that lead to the observed equilibrium state.

The shallow-cumulus boundary layer has been the subject of many research efforts, using a variety of observations, theoretical models, and general circulation models. Several equilibrium models have been formulated for marine cloudy boundary layers, for stratocumulus [22,32] as well as for shallow cumulus [1,8,9]. The emergence of large-eddy simulation (LES) modeling has greatly contributed to shallow-cumulus research, as it provides a high-resolution 3D representation of the boundary layer, explicitly resolving the most energetic scales of motion. An intriguing result of LES research has been the robustness of the shallow-cumulus mass flux, cloud fraction, and surface fluxes to model formulation and resolution [12,33,37]. This robustness suggests that some mechanism exists that is efficient in pushing the system to a certain equilibrium state [19].

This study has as its aim the identifcation and modeling of the dominant feedbacks that lead to the observed equilibrium state of the shallow cumulus boundary layer. While shallow-cumulus research has typically focused on processes in the cloud layer, the interaction of this type of convection with the subcloud mixed layer [8] has received less attention. Yet it can be argued that this interaction is key to establishing the equilibrium state. The balance in the mixed-layer budgets of temperature and humidity is, with constant large-scale forcings, mainly controlled by only two processes: the surface flux and the convective flux at cloud base. The surface flux is usually formulated in a bulk approach, which simply acts to restore the subcloud humidity and temperature to the values at the surface on a time scale set by the speed of the surface wind and the depth of the subcloud layer. This passive behavior implies that the main process that is actively responsible for setting the final equilibrium balance must be convection. Accordingly, this justifies focusing our attention on cloud base convective flux in particular.

In recent decades decades several important findings have been made that are relevant for our purposes. The mass-flux approach [7,30,40] has been shown by Siebesma and Cuijpers [33] to effectively capture the cloud-base convective flux in shallow cumulus. The mass flux is by definition the product of a vertical velocity scale and a convective area-fraction. Observational data [27] and numerical results [18,24] have shown that the relevant vertical velocity scale at cloud base is the convective vertical velocity scale of the subcloud layer [16]. The Gaussian statistical formulation [36] is successful in reproducing LES cloud fractions at the cloud base [14]. Here, knowledge is required of the local saturation deficit as well as the second statistical moment of turbulence, the variance. At a mixed-layer top the latter scales [25] with properties of the cloud-base transition layer [1,5,41], in particular the local vertical gradients, the cloud-base convective flux, and the turnover time scale of the subcloud layer.

This study presents a new equilibrium model for a marine shallow-cumulus-topped mixed layer in which some of these recent insights are combined. The system of equations is closed using a formulation for the mass flux in which the area fraction of the active, surface-driven cloudy thermals is retained [11,24]. Letting the area fraction depend on the state of the system (as opposed to a constant) introduces feedbacks that better maintain the height of the mixed layer near cloud base. The area fraction is modeled using a statistical formulation as a function of humidity and variance at the mixed-layer top. It will be shown that these feedbacks help determine the character of the equilibrium. Comparison to observations, LES, and reanalysis data shows that the shallow-cumulus mass flux, convective area-fraction, cloud-base height, mixed-layer thermodynamic state and variances, and surface fluxes associated with this equilibrium are realistic. In order to optimize transparency, only a simplified boundary layer scenario is studied. This is sufficient to reveal the mechanisms of interest.

The rest of the paper is organized as follows. In Sect. 2 the model is formulated. In Sect. 3 the details of the large-scale forcings, boundary conditions, and constants that are used to solve the model are given. In Sect. 4

the model is solved at a single point using a shallow-cumulus case designed for LES, and over a field of forcings derived from the 40-year reanalysis of meteorological data by the European Centre for Medium-range Weather Forecasts (ECMWF). The results are evaluated against LES results as well as observed trade-wind climatology of shallow-cumulus occurrence and cloud-base height. A time-series analysis is performed to illustrate the relaxation toward equilibrium, revealing the role of the new humidity mass-flux feedback in this process. This mechanism is put in the context of previous equilibrium models for shallow cumulus [1,8]. Finally, the mass-flux model is implemented in an intermediate complexity climate model in which it is fully coupled to and interactive with larger-scale dynamics. The model used for this purpose is the Quasi-equilibrium Tropical Circulation Model (QTCM, see [23]). In Sect. 5 the implications of the results are further discussed, and in Sect. 6 the conclusions are summarized.

2 Model formulation

Figure 1 shows a schematic view of the atmospheric boundary layer, featuring a well-mixed subcloud layer topped by a conditionally unstable shallow-cumulus cloud layer. These layers are defined by the vertical stucture of the mean profiles of liquid water potential temperature θ_l and total specific humidity q_t [7]. Between the two layers, $\{q_t, \theta_l\}$ exhibit a small jump associated with the transition layer, situated in between mixed-layer top and cloud-base height. This transition layer at cloud base is typically observed in the vertical structure of shallow-cumulus-topped boundary layers, especially in the humidity profile [1,5,41]. Surface values are indicated by the superscript s, mixed-layer values by 1, cloud-base values by b, and free tropospheric values by $+$. Various physical processes affecting the mixed-layer humidity, heat, and mass budgets are represented in the figure.

2.1 Subcloud mass budget

Mass conservation in the steady-state mixed layer below the clouds can be expressed as

$$\frac{\partial h}{\partial t} = E + w - M = 0,\qquad(1)$$

where h is the height of the mixed layer, w is the large-scale vertical velocity at h (positive upwards), E is the top entrainment velocity, and M is the shallow-cumulus mass flux at h. Tendency w represents the loss of mass due to lateral outflow at the column edges by low-level divergence of the large-scale winds, pushing down the stable transition layer at h. Integrating the divergence of the horizontal winds D over the mixed layer implies
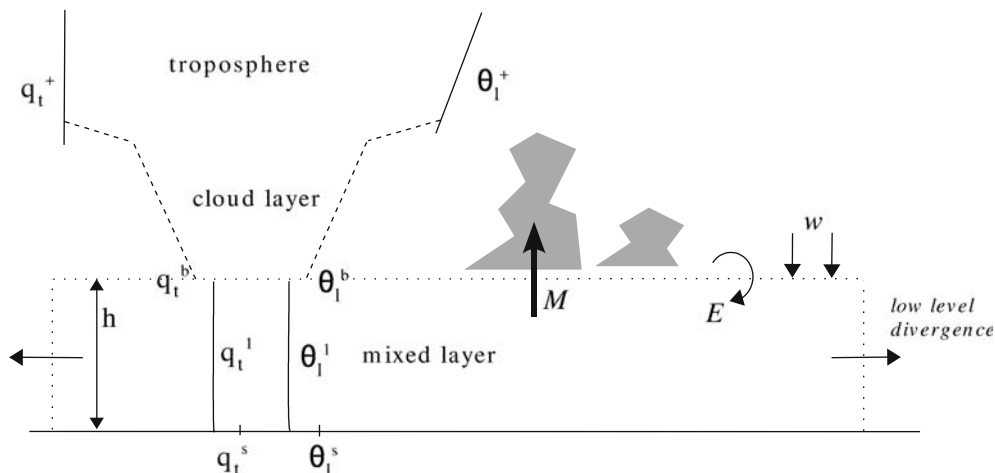
$$w = -D h;\qquad(2)$$

Fig. 1 An idealized view of a shallow-cumulus-topped mixed layer. The *symbols* are explained in the text

see [38] for a detailed derivation and approximations. The cumulus mass flux M acts as a sink term in the mixed-layer mass budget. In contrast, E is a source term, representing the process of engulfment of cloud-layer air into the mixed layer. Equating the buoyancy flux $\overline{w'\theta_v'}$ at h as the product of E and the vertical jump in virtual potential temperature $\theta_v = \theta(1 + 0.61q_t - 1.61q_l)$ gives

$$E = -\frac{\overline{w'\theta_v'}\big|_h}{\Delta\theta_v} = \frac{0.2\,\overline{w'\theta_v'}\big|_s}{\Delta\theta_v}. \tag{3}$$

The script h refers to the mixed-layer top, while $\Delta(..) = (..)^b - (..)^1$ denotes the jump across the transition layer. Here the buoyancy flux at h is equated as a fixed negative factor of the surface buoyancy flux. Equation (3) is the standard definition of top entrainment for dry convective boundary layers and is shown by [33,37] to be similar in the presence of shallow cumulus clouds. This is due to the rising moist updrafts having thermodynamic properties that are still close to those of the mixed layer. Finally, $\Delta\theta_v$ can be expressed in terms of $\{\Delta q_t, \Delta\theta_l\}$:

$$\Delta\theta_v = \Delta\theta_l + 0.61\left(q_t^1\Delta\theta_l + \theta_l^1\Delta q_t + \Delta q_t\Delta\theta_l\right), \tag{4}$$

where it is assumed that no liquid water exists in the (cloud-free) areas where top entrainment occurs. This relation illustrates that typically both jumps contribute oppositely to stability.

In steady-state situations, the mixed-layer height h is such that top entrainment exactly balances the loss of mass by cumulus mass flux and large-scale divergence. Shallow-cumulus cloud-base height in the trade winds is observed to be typically robust and rather constant at about 500–700 m but to gradually increase along the trade-wind trajectory toward the tropics [31].

2.2 Simplified budget equations

The subcloud layer is assumed to be well mixed for temperature and humidity. The most important sources and sinks in their budgets in the mixed layer are the surface flux, the flux at the mixed-layer top, the large-scale forcings, and, in the case of temperature, the radiation [38]. Accordingly, the simplified vertically integrated prognostic budget equations can be written as

$$h\frac{\partial q_t^1}{\partial t} = VC_q^s\left(q_t^s - q_t^1\right) + E\Delta q_t + hF_{\mathrm{adv}q_t}, \tag{5}$$

$$h\frac{\partial\theta_l^1}{\partial t} = VC_\theta^s\left(\theta_l^s - \theta_l^1\right) + E\Delta\theta_l + hF_{\mathrm{adv}\theta_l} + hF_{\mathrm{rad}}. \tag{6}$$

Here, V is the horizontal wind speed close to the surface, and C_q^s and C_θ^s are the bulk transfer coefficients at the surface. The F terms stand for large-scale forcings, where adv indicates horizontal advection and rad radiative processes.

The downward flux at the mixed-layer top in Eqs. (5) and (6) is formulated as the product of the entrainment velocity scale E times the jump in humidity and temperature between the mixed layer and the cloud layer. This jump is assumed here to be a function of the total difference between the mixed layer and the free troposphere:

$$\Delta q_t \approx C_q^c\left(q_t^+ - q_t^1\right), \tag{7}$$

$$\Delta\theta_l \approx C_\theta^c\left(\theta_l^+ - \theta_l^1\right), \tag{8}$$

where the superscript $+$ indicates the free tropospheric value overlying the boundary layer. The coefficients C_q^c and C_θ^c are transfer coefficients that essentially parameterize the cloud layer, representing the efficiency of downward transport of free tropospheric air. Equations (7) and (8) represent a simple linear model for this process, ensuring that the air entrained into the mixed layer is still affected by the properties of its original mixing source, the trade-wind inversion. The coefficients are consistent with a mixing-line model of the cloud layer (e.g., [9]) in which case one would expect that $C_q^c = C_\theta^c$. Differences between the two coefficients can be justified as a result of differential advection of temperature and moisture within the cloud layer, as well as the effect of radiative cooling or other diabatic processes. In this work, we use LESs of the Barbados Oceanic and Meteorological Experiment (BOMEX) [20,28] and the Atlantic Trade-Wind Experiment (ATEX) [4,5] to specify a range of acceptable values (Sect. 3) and adjust within this range to achieve good results. The sensitivity of our results to the magnitude of these coefficients is explored in a companion paper [38], which finds,

as do we, that the net mass flux out of the layer is the principal dependence of the model to its value. As will be shown later, even with constant C^c values this simplified model is able to reproduce the observed spatial variability of subtropical trade-wind cloudiness. This approach is justified for the main purpose of this study, which is to explore the degree to which subcloud mixed-layer budgets alone can explain this observed cloud climatology.

The appearance of E in the budget Eqs. (5) and (6) reflects the fact that mass transport by M and w conceptually does not change mixed-layer humidity and potential temperature. Extraction of air out of the well-mixed bulk layer does not affect the average over the remaining air. Accordingly, only top entrainment of air out of the overlying cloud layer into the mixed layer and the subsequent mixing process can change q_t^1 and θ_l^1. However, note that the mass flux and large-scale subsidence still appear in the model in the mass budget (1).

2.3 Mass-flux closure

In order to complete the system of prognostic Eqs. (1), (5), and (6), the cumulus mass flux M must be parameterized. The commonly used mass-flux approach [7] states that the turbulent flux by cumulus can be well approximated by

$$\overline{w'\phi'} = M \left(\phi^{\mathrm{up}} - \overline{\phi} \right). \tag{9}$$

Here ϕ denotes $\{q_t, \theta_l\}$, the superscript up indicates the air of the rising moist updrafts, and the vertical bar denotes a horizontal average. The mass flux M is the product of an area fraction and a velocity scale,

$$M \equiv a^c w^c, \tag{10}$$

where a^c is the area fraction of the transporting cloudy thermals and w^c is their vertical velocity scale. For simplicity the air density ρ is assumed to be constant, $\rho = 1 \ \mathrm{kg \ m^{-3}}$.

The average vertical velocity over all buoyant, cloudy thermals (called the "cloud core") was shown by [24] to scale well with the Deardorff convective velocity scale w^*, defined as

$$w^c \approx w^* \equiv \left(\frac{g \, h}{\Theta_v^0} \left. \overline{w'\theta_v'} \right|_s \right)^{1/3}. \tag{11}$$

The surface buoyancy flux $\left. \overline{w'\theta_v'} \right|_s$ can be expressed in terms of the surface heat and moisture fluxes [15], which in the bulk aerodynamic formulation are a function of q_t^1 and θ_l^1.

Based on GATE observations Nicholls and LeMone [27] suggested that M is proportional to w^*. The same conclusions are drawn by Grant [18] from a TKE budget analysis in LES, introducing a constant of proportionality 0.03. However, retaining the area fraction a^c in the mass-flux closure instead of a constant permits one to distinguish between conditions where a larger or smaller fraction of the active mixed-layer thermals associated with w_* actually condensate (i.e., reach their lifting condensation level, or LCL), and thus contribute to M [24]. This connection with mixed-layer humidity could be essential in enabling a realistic equilibrium solution for this system of equations. As a first-order guess for the moist convective area-fraction at the top of the mixed layer, a simplified version of the statistical cloud fraction parameterization of [15] is used that only acts on moisture,

$$a^c = 0.5 + \beta \, \mathrm{Atan} \left(\gamma \frac{q_t^1 - q_{\mathrm{sat}}}{\sigma_q} \right), \tag{12}$$

where q_{sat} is the saturation specific humidity and constants $\beta = 0.36$ and $\gamma = 1.55$ represent the fit of this function to LES results as proposed by [14]. The ratio between the brackets is the normalized saturation deficit, or the distance from saturation normalized by the turbulent variance. Since this cloud fraction is used in the mass flux, it includes only cloudy points that contribute to vertical transport. Any passive cloudiness would have to be treated separately. The typical shape of Eq. (12) is shown in Fig. 2a, and the corresponding PDF of humidity in Fig. 2b.
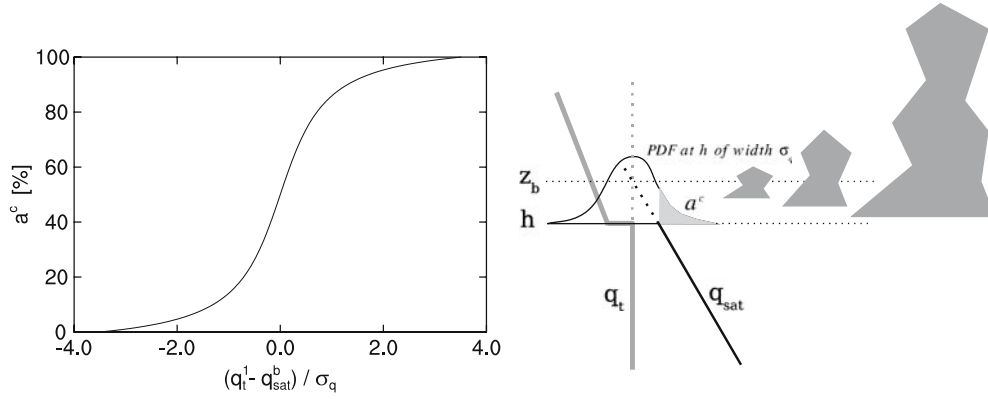
Fig. 2 a Area fraction closure Eq. (12) as function of normalized saturation deficit. **b** Corresponding shape of PDF of q_t (*thin solid black line*). a^c corresponds to the fraction of the PDF that lies above the saturation curve (*shaded light gray*). Cloud-base height z_b is defined here as the height at which 50% of the PDF (all updrafts) would have been saturated

2.4 Variance budget

While q_t^1 and q_{sat} are simple diagnostic functions of the model state, closure of σ_q is still required. The variance budget can be written as

$$\frac{\partial \sigma_q^2}{\partial t} = -2\,\overline{w'q_t'}\frac{\partial \overline{q_t}}{\partial z} - \frac{\partial \overline{w'q_t'q_t'}}{\partial z} - \frac{\sigma_q^2}{\tau}, \tag{13}$$

where the terms on the right-hand side represent flux-gradient production, vertical transport, and dissipation, respectively. We now assume that the typical turnover time scale of shallow-cumulus updrafts is relatively small compared to that of the variance storage term, allowing diagnostic calculation of the variance at any time. For the variance dissipation time scale τ the turnover time of the largest subcloud-layer eddies is used:

$$\tau = \frac{h}{w^*}. \tag{14}$$

Variance transport at $z = h$ is assumed to be dominated by advective transport by the strongest subcloud-layer updrafts. Using the typical vertical structure of variance in the subcloud layer, with a minimum at $z = \frac{1}{2}$ and a much larger maximum at $z = h$, the advective transport of variance by updrafts can be estimated as

$$-w_{up}\frac{\partial (\sigma_q^h)^2}{\partial z} \approx -w_*\frac{(\sigma_q^h)^2}{\frac{1}{2}h} = -\frac{(\sigma_q^h)^2}{\tau}. \tag{15}$$

This illustrates that at the mixed-layer top the transport tendency acts as a relaxation term with the same time scale as dissipation, which allows representation of both processes by a single term. Finally, for the production term, the flux at h is assumed to be close to the surface flux, whereas for the local gradient a bulk gradient format is used:

$$\left.\frac{\partial \overline{q_t}}{\partial z}\right|_h \approx \frac{\Delta q_t}{\Delta z}, \tag{16}$$

where Δz is the depth of the transition layer and Δq_t the humidity jump across it, see Eq. (7). Substituting in Eq. (13) and then rewriting finally gives

$$(\sigma_q^h)^2 = -\frac{\left.\overline{w'q_t'}\right|_s}{w^*}\,\Delta q_t\frac{h}{\Delta z}. \tag{17}$$

This scaling for the variance at the mixed-layer top is derived and studied in more detail by [25]. The structure is that of the surface convective humidity scale q^*, multiplied by a factor dependent on properties of the cloud-base transition layer. The transition-layer depth Δz is assumed to be constant for simplicity.

Next to the convective vertical velocity scale w_*, the humidity variance is the second most important parameter that couples the shallow-cumulus mass flux to the subcloud layer turbulence intensity. Equally important is that the cloud-base variance carries transition-layer properties.

3 Forcings and boundary conditions

The model consists of three prognostic equations—Eqs. (1), (5), and (6)—for $\{h, q_t^1, \theta_l^1\}$. The diagnostic variables in the model are $\{E, M, a^c, w^*, q_{\text{sat}}, \sigma_q^h, \Delta q_t, \Delta \theta_l, \Delta \theta_v, \overline{w'\theta_v'}\big|_s, \overline{w'q_t'}\big|_s\}$. What remains are either constants or can be considered large-scale forcings or boundary conditions.

Firstly, the model is solved for an approximately steady-state marine shallow-cumulus case that has been designed for LES. This enables evaluation of the equilibrium model solution for parameters such as the cumulus mass flux and convective cloud fraction, which can only be provided by LESs. The case used here is the Barbados Oceanic and Meteorological Experiment (BOMEX), as described by [20] and [28]. The cumulus clouds were observed to be shallow, and the boundary layer was in steady state. The BOMEX LES intercomparison case is described by [34], and an overview of the input values used here is given in Table 1.

Next the model will be solved on global climatological fields of the forcings and boundary conditions. The global input fields used here are obtained from the ECMWF Reanalysis project (ERA40) archive. The required forcings and boundary conditions are $\{q_t^s, \theta_l^s, q_t^+, \theta_l^+, V, D, F_{\text{adv}q_t}, F_{\text{adv}\theta_l}, F_{\text{rad}}\}$. The fields q_t^s and θ_l^s can be determined given the sea-surface temperature (SST) and the surface pressure (p_s). q_t^+ and θ_l^+ are diagnosed at a level that is always just above the trade-wind inversion (level 47, at ≈ 2 km) in order to avoid the presence of boundary-layer properties in the climatological average. V is the 10 m wind speed, and the large-scale divergence D at level 51 (≈ 0.75 km) is used, which is assumed to be close to the mixed-layer top. Finally, the forcing tendencies $F_{\text{adv}q_t}$, $F_{\text{adv}\theta_l}$, and F_{rad} are obtained at level 55 (≈ 0.3 km). These forcings are especially important for a realistic heat budget as they represent the only cooling term in the subcloud mixed layer (as opposed to the surface heat flux and the convective flux).

What remains is the choice of the constants $\{\Delta z, C_q^s, C_\theta^s, C_q^c, C_\theta^c\}$. These constants are set to typical values obtained from LESs or observations. Δz is set to 100 m [8,25]. The surface bulk transfer coefficients C_q^s and C_θ^s have the typical oceanic value of 0.0012, based on observational data [17] and often used for numerical modelling [3,39]. Cloud transfer-coefficients C_q^c and C_θ^c can be diagnosed in LES from the hourly mean profiles, using Eqs. (7)–(8). Doing so for both BOMEX and ATEX resulted in the typical values 0.1 and 0.03, respectively (Fig. 3). A sensitivity test for these parameters (not shown) also suggested that these particular values give the best overall solution.

4 Equilibrium solutions

The main novelty of this model is that the convective area-fraction in the mass-flux formulation is retained, which introduces an extra degree of freedom in the mass flux, representing new interactions between mixed-layer humidity and the convective transport. Through the mass budget these might help maintain boundary-layer height. As will be illustrated in this section, this humidity dependence of the convective mass flux is essential for a realistic equilibrium state of the shallow-cumulus-topped boundary layer, including temperature and humidity, their surface fluxes, the convective area-fraction and mass flux, and the turbulent variances. The existence of such a solution has been shown by [1,8,9] and has long been suspected based on (a) the observed persistence of shallow-cumulus cloud-occurrence in the subtropical trades [29] and (b) the robustness of the shallow-cumulus mass flux under changes in resolution and subgrid scale models in numerical LESs simulations [19]. By putting the model in the context of previous shallow-cumulus equilibrium models [1,8] it will be shown that retaining a flexible convective area-fraction in the mass flux as a function of humidity is in fact an alternative representation of some essential aspects of these models.

Table 1 Characteristics of BOMEX marine shallow-cumulus case input parameters used to solve equilibrium model

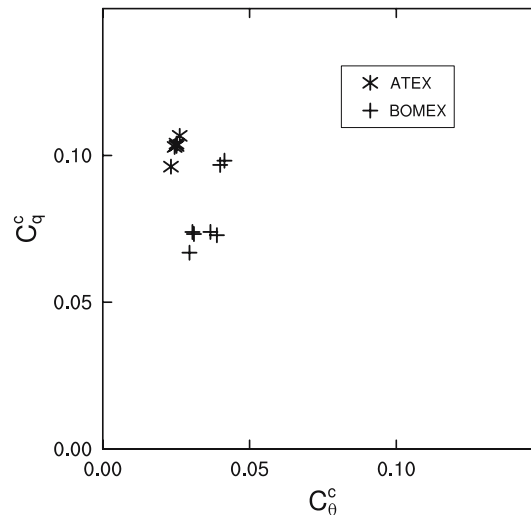| V (m s^{-1})	SST (K)	D (s^{-1})	q_t^+ (g kg^{-1})	θ_l^+ (K)	F_{rad} (K day^{-1})	$F_{\text{adv}\theta_l}$ (K day^{-1})	$F_{\text{adv}q_t}$ (g kg^{-1} day^{-1})	p_s (hPa)
8.75	300.4	4.3×10^{-6}	4.0	308	−2.0	0.0	−1.2	1,015

The LES case description is given by [34]

Fig. 3 Cloud tranfer-coefficients C_θ^c and C_q^c, as diagnosed in LES for the BOMEX and ATEX cases, using Eqs. (7) and (8)

4.1 The BOMEX case

First the model is solved for the BOMEX case using an integration timestep of 60 s. Table 2 shows the model state after 167 h, when it has equilibrated. Included are the mass flux and cloud fraction, cloud-base height, convective vertical velocity scale, cloud-base humidity variance and saturation deficit, and the surface fluxes of heat and moisture. LES results on the same parameters are also given.

The equilibrium state of all free model variables is of at least the right order of magnitude. The surface latent heat flux and boundary-layer height have realistic values. The small convective area-fraction typical for shallow convection is reproduced, as well as the mass flux and variance. The typical scatter in these variables over all LES models in the BOMEX intercomparison case [33] was about 1% in the cloud core fraction and $0.0075 \, \mathrm{ms^{-1}}$ in the mass flux. Judged by those criteria the equilibrium model is doing reasonably well, given that the model only represents an idealized bulk mixed layer. But perhaps it is most relevant to view these results in the context of the typical unsatisfactory performance of many single-column models for these parameters, as documented by several intercomparison studies on such cumulus cases [21].

Apparently the mixed-layer budgets of mass, heat, and humidity can explain the equilibrium state in LES of the structure of the trade-wind boundary layer, in particular the convective mass flux and cloudy area-fraction. An important observation is that the equilibrium state is always close to saturation, with a saturation deficit at h of only a few g kg^{-1}, and a typical cumulus area-fraction of only a few percent. This reflects that the existence of a nonzero mass flux requires the condensation of *at least some* rising thermals due to its dependence on the area fraction.

To further explore the role of this humidity sensitivity of the mass flux, the process of adjustment to equilibrium is now studied for the BOMEX case (Fig. 4). A sensitivity test is done on the initial boundary-layer height to assess stability. Initial mixed-layer humidity is always equal to q_t^+. In addition, to further assess stability, a humidity perturbation of $+1$ g kg^{-1} is applied at $t = 117$ h. The results indicate that the model always reaches a stable state. First the mixed layer deepens by top entrainment as there is no mass flux to

Table 2 Results on BOMEX marine shallow-cumulus case, comparing the simple model to LES

	h (m)	M (m s^{-1})	a^c (%)	w^* (m s^{-1})	σ_q^h (g kg^{-1})	$(q_t - q_{sat})^b$ (g kg^{-1})	L (W m^{-2})	H (W m^{-2})
Model	692	0.032	4.3	0.75	1.00	-2.08	162	6.4
LES	620	0.022	3.5	0.51	0.64	-1.51	150	10

The LES results are averages over a range of different codes as reported by [34], except for the cloud-base saturation deficit and the humidity variance, which were obtained using only the KNMI LES model [14]. The cloud-core fraction in LES is defined as the ratio of the positively buoyant cloudy area to the total area at the cloud-base height
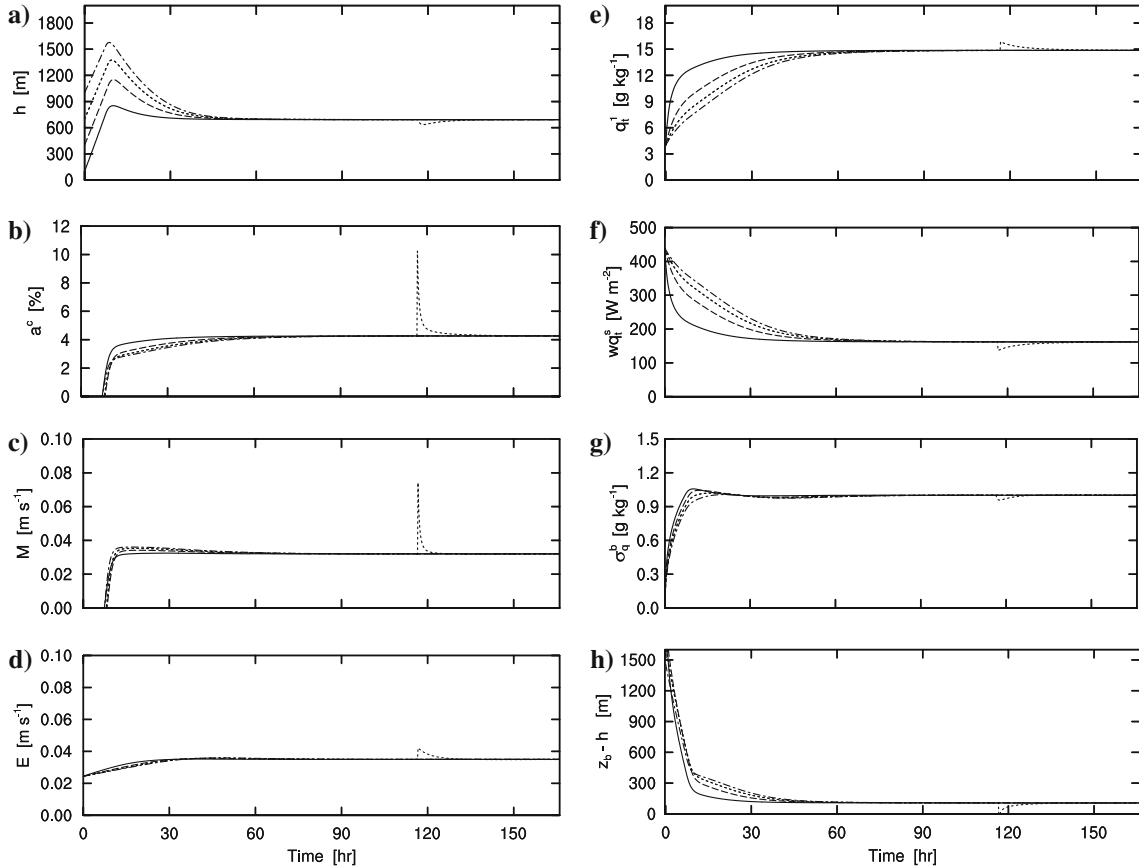
Fig. 4 Time series of some model variables during solution process for BOMEX case. **a** Mixed-layer depth h. **b** Area fraction a^c. **c** Mass flux M. **d** Top entrainment velocity E. **e** Mixed-layer humidity q_t^1. **f** Surface evaporation. **g** Square-root of variance σ_q^h. **h** Distance of h from cloud-base height z_b. Four experiments are shown, with identical initial thermodynamic state $\{\theta_l^1, q_t^1\} = \{\theta_l^s - 2, q_t^+\}$ but with a different initial mixed-layer height h: 100 m *solid*, 400 m *dashed*, 700 m *dotted*, and 1,000 m *dash-dotted*. In one of the experiments a perturbation is added to q_t^1 at $t = 117$ h, when all experiments have equilibrated

compensate it because q_t^1 is still too small. When finally humidity has increased such that some thermals start to reach saturation at h, the mass flux quickly gets large and overcomes top entrainment to reduce h toward its equilibrium value. Full equilibrium is reached after about 100 h, which is comparable to the model of [1].

In contrast to mixed-layer depth and humidity, the area fraction a^c and mass flux M restore very quickly after the mixed-layer humidity perturbation at $t = 117$ h. Mixed-layer height h plays an important role in this negative feedback process, as illustrated schematically in Fig. 5. First, the humidity increase makes more rising thermals condensate at h, equivalent to an increase in a^c. This corresponds immediately to a larger mass flux M. The associated reduction of h through mass budget Eq. (1) affects q_{sat} at h through the associated increased temperature T^h. This quickly increases the saturation deficit again, which in turn restores a^c (and with it M) back to smaller values. After that, h is slowly restored by top entrainment, and humidity is slowly restored by (a) the temporarily reduced surface evaporation and (b) the continuous drying by top entrainment. The only modest reduction in h during the perturbation expresses the robustness of the system for perturbations in humidity.

The importance of this interaction between mass flux, humidity, and mixed-layer height for the boundary-layer equilibrium was already realized by [8] and [1]. In both models cloud-base height z_b is prescribed to be situated close to or at the top of the mixed layer h, a constraint then used for closure of the cumulus mass flux. In contrast, in this model the proximity of h to z_b is not prescribed but is flexible, as a result of the variable saturation deficit at the mixed-layer top. The negative feedback introduced into the mass flux by retaining the area fraction always acts to automatically bring h to a height where a certain fraction of rising thermals condensates, so that M exactly balances E and w in the mixed-layer mass budget. This means that
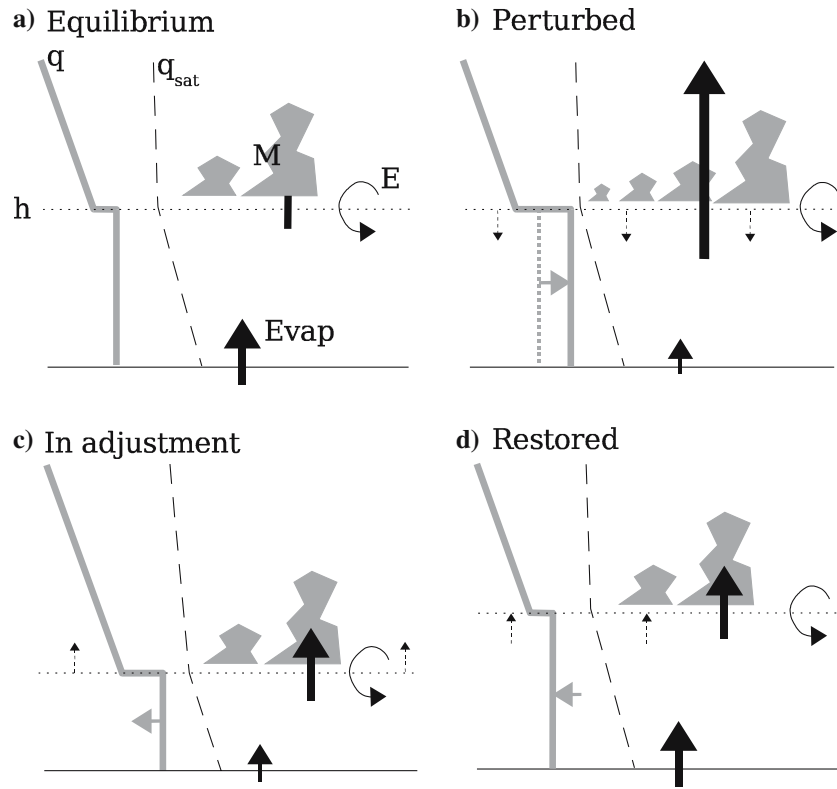
Fig. 5 Schematic illustration of feedback mechanisms between mixed-layer humidity, convective mass flux, and mixed-layer height. **a** System in equilibrium. **b** State immediately after positive humidity perturbation, which through a^c yields a larger M, which through the mixed-layer mass budget Eq. (1) causes a fast decrease in h. **c** Adjustment stage in which M is restored but mixed layer slowly gains mass by entrainment. **d** Fully restored equilibrium state. The *symbols* are explained in the text

the mixed-layer top will always end up close to cloud base, or, in other words, the system automatically seeks a certain close proximity to saturation at the top of the mixed layer.

This behavior is further illustrated by the time series of the distance of h from the cloud-base height z_b. Although the latter is not a model variable, it can be represented by the height at which all updrafts would have reached their LCL or, in other words, where 50% of the PDF would be crossing the saturation curve (Fig. 2b). This gives

$$z_b - h = \frac{q_t^1 - q_{\text{sat}}^h}{\partial_z q_{\text{sat}}}, \tag{18}$$

where $\partial_z q_{\text{sat}}$ is the gradient of the saturation specific humidity in the mixed layer. Figure 4h shows that while before cloud onset h can be situated far below cloud base, afterwards it is always only within a few hundred meters. Accordingly, the nonconstancy of the convective area-fraction in the mass flux is an alternative but more flexible expression of the constraint used by [1,8] for mass-flux closure. The extra degree of freedom in the mass flux represented by the area fraction thus acts as a regulator or "valve" on convective transport [11], dependent on bulk mixed-layer humidity conditions.

It is possible to estimate the associated adjustment timescales. In absence of cloudy mass flux the relevant time scale of the mass budget is

$$\tau_E = \frac{h}{E} = \frac{h}{w} = \frac{1}{D}, \tag{19}$$

e.g., [37]. Using BOMEX values gives $\tau_E = 2.5 \cdot 10^5$ s, about 70 h. This is the time associated with the creation of a mixed layer by top entrainment and can be identified in Fig. 4 as the typical time scale of adjustment of h to equilibrium after initialization and of its restoration by entrainment after perturbation. The time scale of the sudden drop in cloud-base height h' by M during the humidity perturbation is

$$\tau_M = \frac{h'}{M}. \tag{20}$$

Estimating $h' \approx 100\,\text{m}$ and $M \approx 0.1\,\text{m s}^{-1}$ from Fig. 4 gives $\tau_M = 1000\,\text{s}$. This is on the order of a single eddy turnover time scale, defined as $\tau_{\text{eddy}} = h/w_*$. Comparing τ_M to τ_E shows that the mass flux acts much faster on h than the slow adjustment by top entrainment. This reflects the strong sensitivity of the mass flux to humidity through the area fraction and the associated strong impact on the mixed-layer mass budget. In Fig. 4 this is evident in the fast growth in M after cloud onset at $t = 10\,\text{h}$ and its relatively strong perturbation at $t = 117\,\text{h}$.

4.2 ERA40 global fields

Next the model is solved over ocean points given the global ERA40 climatology of the boundary conditions and forcings, for the month of July. This should reproduce the characteristic spatial structure and distribution of the shallow-cumulus mass flux and cloud fraction. Note that the solution of the equilibrium model will only make sense in the regions where climatology is typically dominated by shallow-cumulus convection. Naturally, the subtropical oceanic trade-wind regions are the prime example, and accordingly the evaluation of the model solution will be focused on these areas. In areas where precipitation or radiative cloud top cooling play an important role, the model does not capture all necessary physics, such as the intertropical convergence zone or the stratocumulus regions, respectively. Furthermore, the model will only be solved on gridpoints that have large-scale subsidence, as the small jump at h has to be maintained. Finally, the model solution will only be calculated over the oceans, as over the continents the shallow-cumulus boundary layer is typically not in steady state but experiences a strong diurnal cycle.

Figure 6 shows the equilibrium solution of the thermodynamic state variables q_t^1 and θ_l^1. Mixed-layer temperature and humidity in the subtropics increase toward the equator due to the increasing SST and
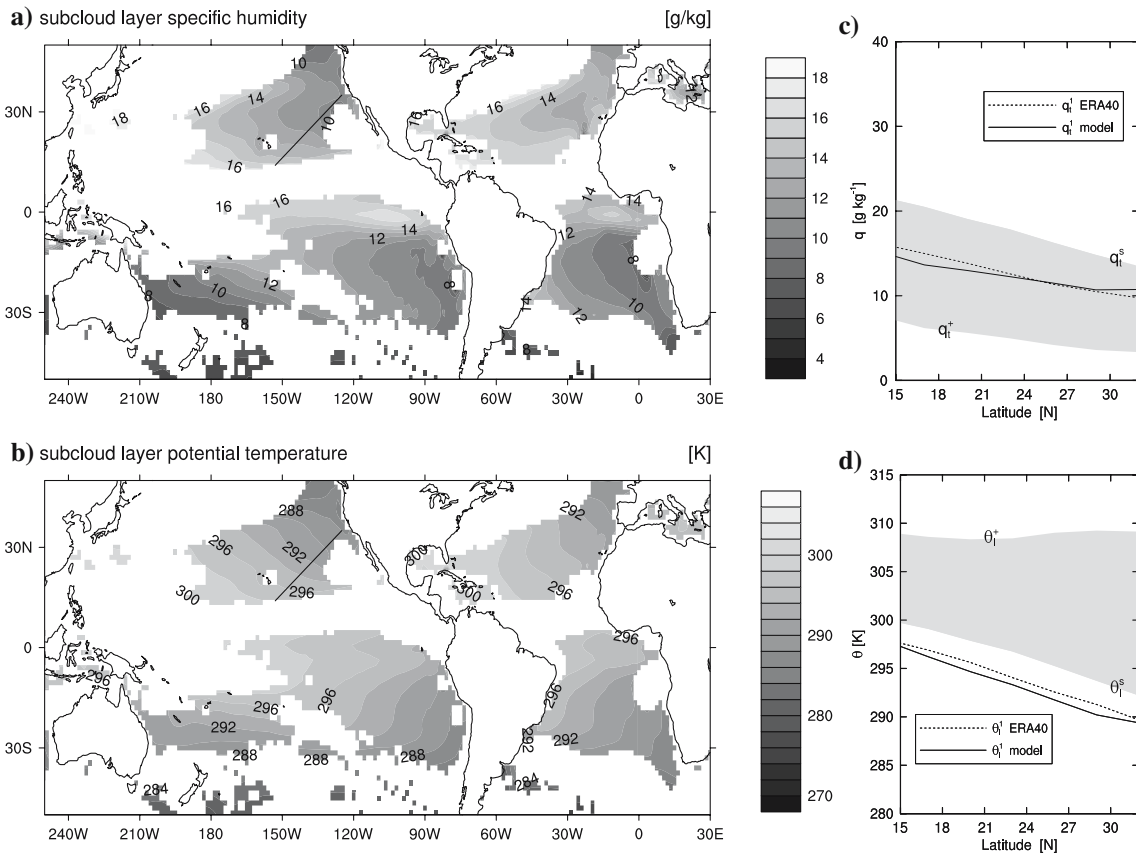

Fig. 6 Equilibrium solution with ERA40 July forcings and boundary conditions of subcloud layer thermodynamic state, with **a** total specific humidity q_t^1 and **b** liquid water potential temperature θ_l^1. **c, d** Cross-section through **a** and **b** along the northeastern Pacific trade-wind trajectory (*dark line*). The boundary conditions at the surface and free troposphere are also shown (the range between these values is shaded *gray*), as well as ERA40 climatology of the solution variables (averaged over mixed-layer depth)

tropospheric humidity. The solution is also plotted on a cross-section approximately aligned to the low-level trade winds in these areas (Fig. 6c,d). This cross-section is the same as used in the European Cloud-System Studies (EUROCS) intercomparison project for general circulation models on clouds in this area, as described by [35]. In general, the subcloud mixed-layer temperature and humidity closely follow the ERA40 climatology. While q_t^1 is always enveloped between q_t^s and $q_t^\top$, θ_l^1 is always lower than the surface value. This reflects the fact that, while for humidity the surface and top flux act as a source and sink, respectively, they are both a source term for temperature. This is characteristic of convective mixed layers that are only cooled by radiation and large-scale advection, an aspect reproduced by the model everywhere.

The surface fluxes of sensible and latent heat are a critical indicator of model performance, as they act on small differences of temperature and humidity, respectively. Figure 7a and b shows the solution fields of the surface latent and sensible heat flux. The surface evaporation increases along the trade-wind trajectory while the sensible heat flux field is much flatter, with a maximum near Hawaii. Figure 7c and d shows that, notwithstanding a mean bias, the spatial structure of the reanalysis surface latent and sensible heat fluxes is reproduced satisfactorily. The underestimation could be due to (a) simplifications in the model or (b) transients in the reanalysis fields (e.g., deep convective events or surface wind bursts), not captured by the shallow-cumulus model but possibly responsible for increasing the time-average surface fluxes in the reanalysis. Nevertheless, most important is that the agreement on the general spatial structure is significant, see also Fig. 8.

The equilibrium solution of the cloudy state is shown in Fig. 9a–c. The solution fields are relatively smooth. The cloud-base height is robust, always at about 400–800 m, but slowly increasing along the trade-wind trajectory. This is in agreement with the radiosonde observations as presented by [31] (Fig. 9g). Along the trade-wind trajectory the convective area-fraction and mass-flux fields gradually increase, from relatively small values upstream toward typical trade-wind values further downstream.

Observations of cloud climatology in the trades are typically only available in the form of frequency of occurrence, for example as obtained from in situ surface observations [29]. There is no simple relation between
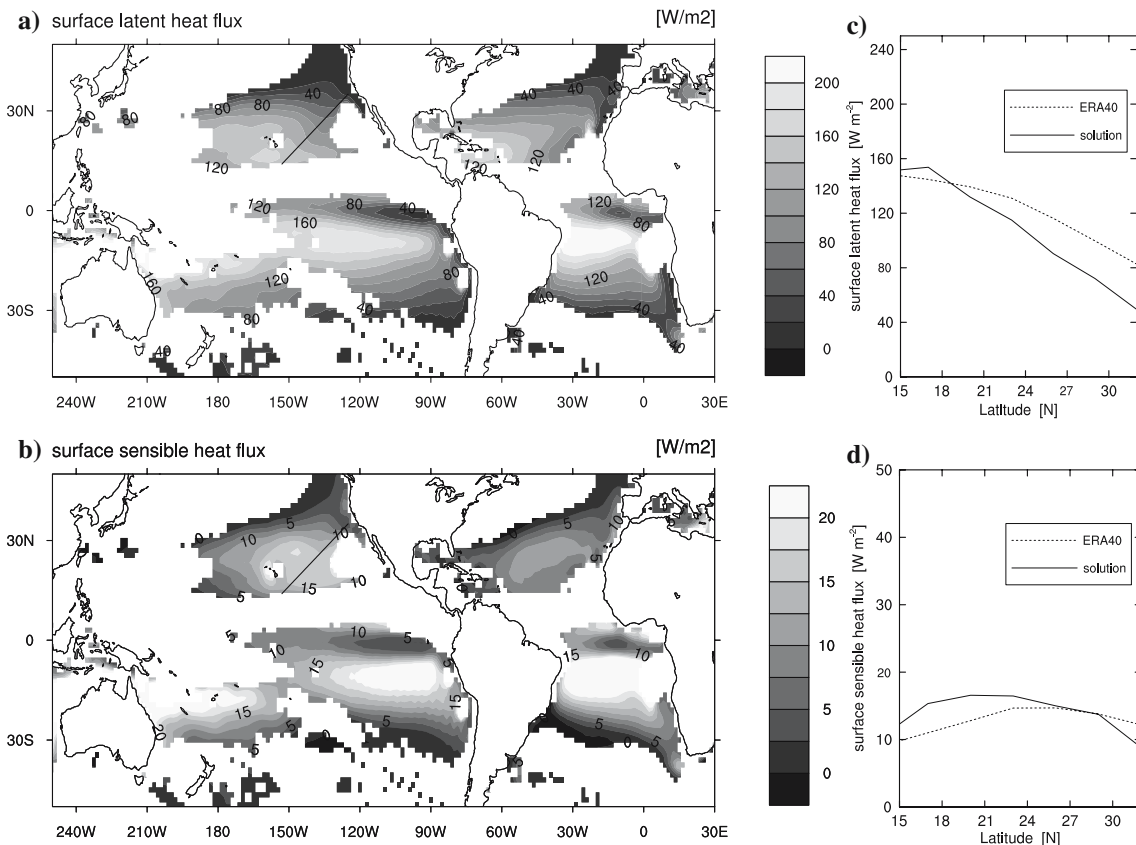

Fig. 7 Equilibrium solution with ERA40 July forcings and boundary conditions for **a** surface latent heat flux and **b** surface sensible heat flux. **c, d** Cross-section through panels **a** and **b** along northeastern Pacific trade-wind trajectory
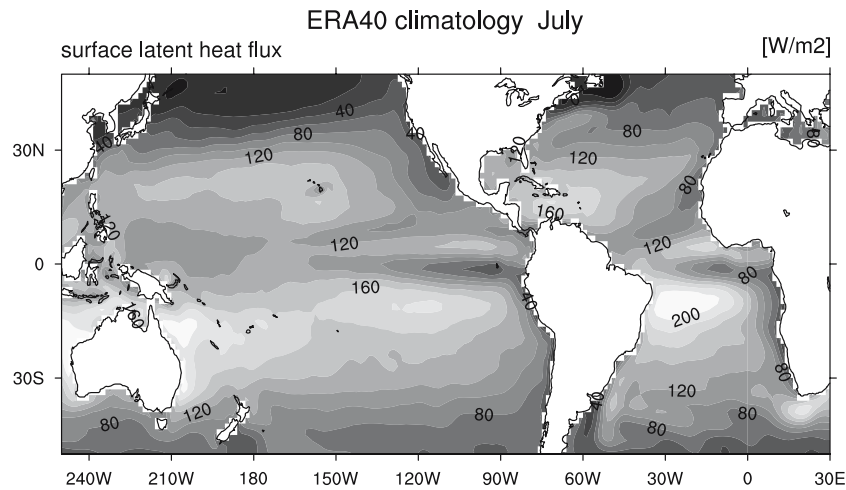
Fig. 8 ERA40 July climatology of surface latent heat flux. Land area has been masked for convenience

ship-observed frequency of occurrence and area fraction. Qualitatively, however, regions of higher or lower frequency of occurrence should correspond to larger or smaller area fraction. At this qualitative level, the spatial structure of the two time-averaged signals can still be compared. Comparing Fig. 9b to the observed 40-year climatology of shallow-cumulus cloud-occurrence as published by Norris (Fig. 5 of [29]) reveals that good agreement exists on the basic features of the field, such as the slowly increasing shallow-cumulus activity along the trade-wind flow. Considering the areas where a solution is calculated, the location of the maxima in the four trade-wind regions of the northern and southern Atlantic and Pacific Oceans correspond well.

The nature of the increasing cloud fraction (and mass flux) along the trade-wind trajectory (Fig. 9d) can be explored more thoroughly. Figure 9e and f shows the two variables that determine the area fraction. Along the trajectory the humidity variance σ_q^2 increases while the saturation deficit increases too. This corresponds to a drier but more vigorously turbulent subcloud layer. Apparently stronger variance overcomes the effect of the lower relative humidity, which leads to the increasing area fraction. This turbulent structure is needed for the equilibrium between boundary-layer convection and the large-scale forcings and boundary conditions to be established. This is an important new aspect of the model, which results directly from the use of a statistical closure for the convective area-fraction.

4.3 An interactive climate experiment

The results so far have shown that the formulation of the mass-flux closure yields a realistic equilibrium. This feature makes the closure attractive for application in convection schemes for general circulation models. The question of how this mass-flux model behaves when fully interactive with the larger scales has not yet been addressed. Many studies of new parameterizations skip the step of evaluation in fully interactive mode with the larger-scale flow. As a result, these parameterizations may produce unexpected behavior when applied in GCMs. As a useful first step in testing such interactions between subgrid-scale physics and the larger scales, the shallow-cumulus mass-flux scheme of Eqs. (9)–(17) is implemented in an intermediate complexity tropical climate model. A climate run is performed, and the results are compared to the diagnostic solution of the model and the observations as discussed earlier.

For these purposes we use the Quasi-equilibrium Tropical Circulation Model (QTCM), as formulated by [23]. This is an intermediate complexity model featuring some key assumptions on the vertical structure of the tropical atmosphere. The resulting reduced number of degrees of freedom in the governing equations makes time integration fast and physical processes more transparent. This is convenient for studying the interaction of experimental boundary-layer convection schemes with large-scale circulation.

Compared to the standard model as described by [23], the model has been equipped with an extra degree of freedom for humidity, representing an atmospheric boundary layer of constant depth. The associated de-coupling of boundary layer and free tropospheric humidity is controlled by the local intensity of atmospheric convection. The Betts–Miller scheme for deep convection as used in the standard model is expanded to cover shallow convection as well, using a flexible shallow adjustment time scale dependent on the local mass-flux
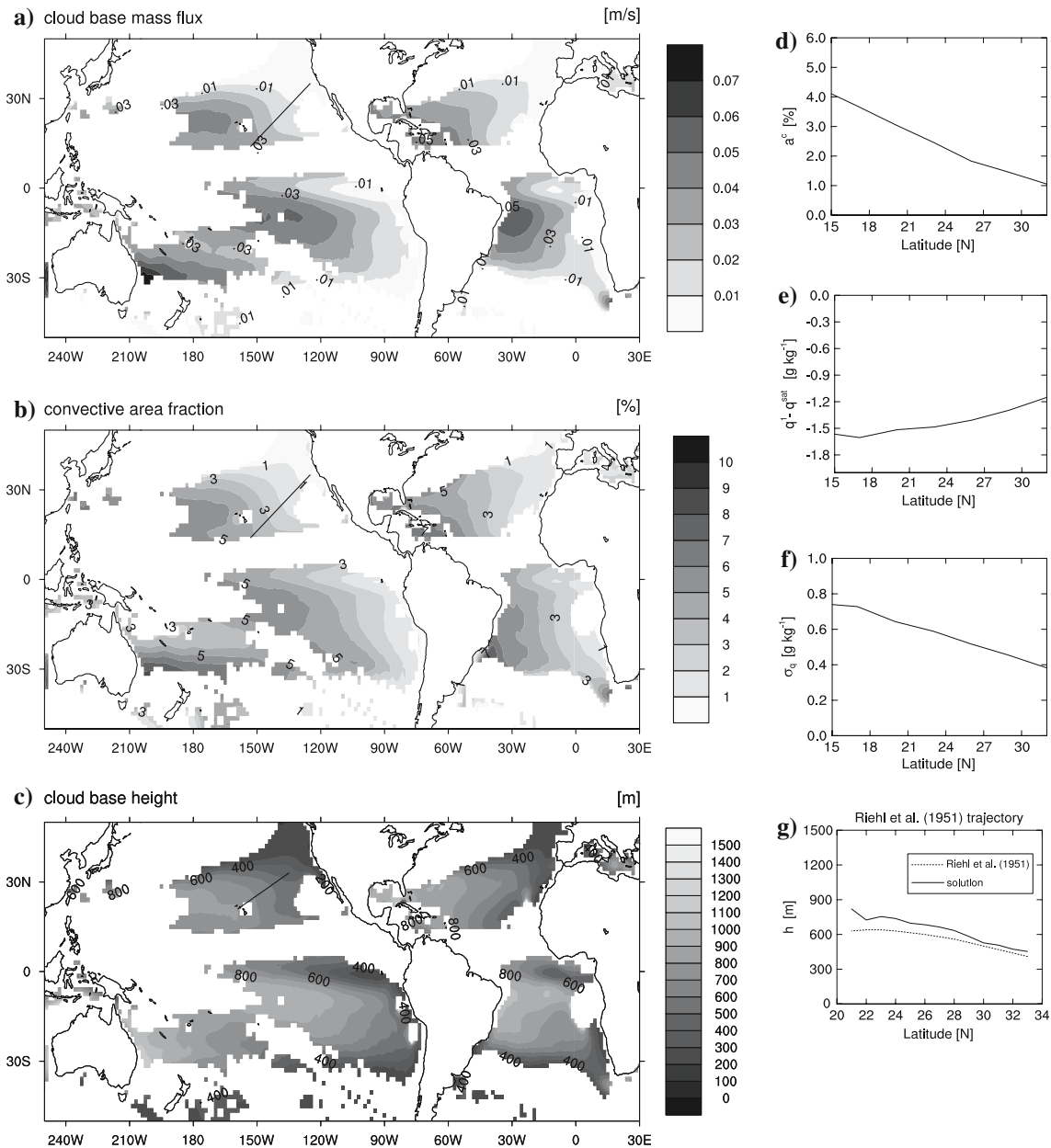
Fig. 9 Equilibrium solution with ERA40 July forcings and boundary conditions of cloud state at cloud base for **a** mass flux, **b** convective area-fraction, and **c** cloud-base height. **d**–**g** Cross-section along northeastern Pacific trade-wind trajectory of **d** convective area-fraction a^c, **e** saturation deficit, **f** square root of humidity variance σ_q^h, and **g** cloud-base height. The latter is shown on a slightly differently oriented cross-section in order to compare to the cloud-base height observations of [31] (*dotted line*)

intensity. The latter is parameterized using Eqs. (9)–(17). Details of the modified QTCM and its shallow convection scheme are described by [26].

In larger-scale models, knowledge of where the cumulus regime is active is required before any convection model can be applied. This is sometimes referred to as the "cumulus triggering" problem. In this model the flexibility of the moist area fraction a^c, on which the mass flux is dependent, in effect already represents a "soft" triggering function; shallow cumulus is active whenever $a^c > 0$ ($M > 0$). A strict regime separation, which is often reported to be the cause of problems in larger-scale models, is thus avoided: the transition between cumulus and noncumulus regimes can become gradual, controlled by the development of a^c. This feature is further illustrated in the next section by a sensitivity test for the larger-scale divergence (Fig. 11).

A climate run of 17 years is performed using observed SSTs from 1981 to 1998. Figure 10 shows the resulting monthly mean July climatology of the QTCM shallow convective area-fraction. The structure of the field is similar to the observed frequency of occurrence [29] and the equilibrium model solution (Fig. 9b). As for the equilibrium model, the QTCM implementation does not apply the shallow-cumulus scheme in convective precipitative conditions, in which the standard Betts–Miller scheme is used. The mean 70-W m^{-2} contour, marked in the figure, encloses the area where the equilibrium solution is often not relevant. Note that this area is oriented somewhat differently compared to Figs. 6, 7, and 9 due to the presence of transients on weather-system time scales, yielding alterations between precipitation and shallow convection. There are also slight differences in climatology of convergence in the QTCM compared to ERA40. Nevertheless, the good agreement between the interactive experiment and the diagnostic experiment on the cloud fraction in the solution areas shows that in an interactive mode the mass flux model retains its favorable behavior. It does not cause instability in the larger-scale model but is stable, always keeping the boundary-layer state close to the observed equilibrium state for long climatological time scales. For a detailed QTCM study of the impact of shallow-cumulus convection on tropical climate system dynamics we refer the reader to [26].

5 Discussion

To gain further insight into the model, we explore its behavior as a function of large-scale divergence, increasing D from very large values that might be characteristic of offshore clearings during Santa Ana conditions in southern California, to much smaller values as might be expected through the trade-wind regimes. Other forcings are characteristic of values taken from BOMEX, as a proxy for typical trade-wind values.

Results showing the convective area-fraction, PBL depth, entrainment, and mass flux as a function of D are presented in Fig. 11. For sufficiently large divergences cloud-free solutions are possible; in such situations the cloud-free mass balance $h = E/D$ can be satisfied for sufficiently small values of h to prohibit condensation at the top of the layer. Because E is a rather weak function of the surface fluxes (scaling with the third power of the surface buoyancy flux), decreasing D is principally balanced by increasing h. When h begins to approach the LCL of mixed-layer thermals, clouds act to enhance the ventilation of the cloud layer, thereby mitigating the rise in h, through an increase in M, as D is decreased further. Because, like E, M scales with w_* and hence is only weakly dependent on surface buoyancy fluxes, any increase in M must be accompanied by increasing convective area-fractions. This highlights the valvelike nature of the closure in Eq. (12). Because M reduces h but has little effect on the LCL, a too rapid rise of h (relative to the LCL) as a function of external parameters must be balanced by an increased saturation deficit ($h - LCL$) and hence cloud fraction, an effect that is robustly captured by our model in Eq. (12).

Although not shown, these solutions also exhibit a tendency for the latent heat fluxes to increase with a^c as D decreases. Such behavior is also evident in the more general solutions as presented in Figs. 7a and 9a. Why?
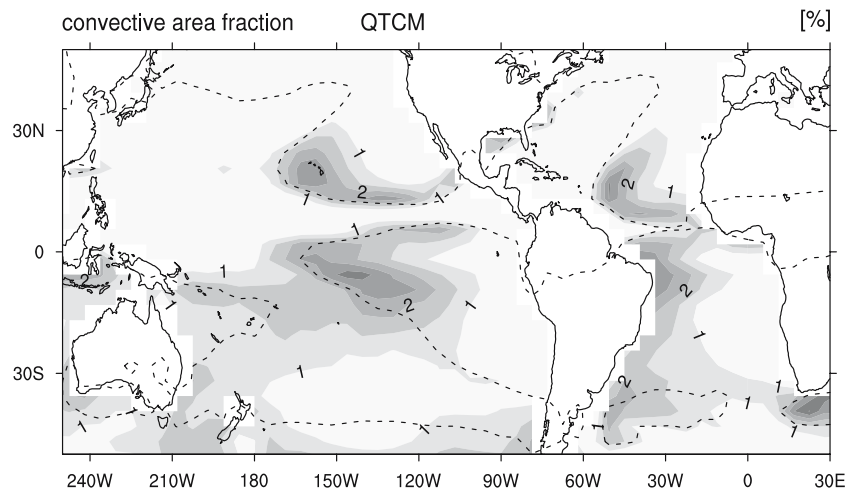

Fig. 10 July shallow-cumulus convective area-fraction (%) of QTCM climate run featuring shallow convective mass-flux scheme Eqs. (9)–(17). The climatological monthly mean for July is shown. *Dotted line*: 70-W m^{-2} precipitation rate isoline, enclosing area where precipitating deep convection dominates in QTCM

Here we note from Eq. (5) that for a fixed advective forcing, the equilibrium surface moisture flux scales with the advective forcing times the depth of the mixed layer. In other words, the efficiency of advective drying vs. surface moistening scales with the depth of the layer; hence in both respects an increasing a^c and an increasing latent heat flux are a byproduct of the model's equilibria being characterized by a deeper subcloud layer. Some of these issues are explored further by [37] (this volume), where for the limiting case of fixed free-tropospheric temperatures and $C_q^c = C_\theta^c$ some insights can be gained analytically. One result of this analysis is to show that the cloud transfer coefficients play a critical role in setting the convective area-fraction but are secondary in the determination of the surface fluxes, which might explain why for our chosen values of C_q^c and C_θ^c reasonable solutions for M and a_c could be obtained even when surface latent heat fluxes were in places less well represented.

The sensitivity study presented with the help of Fig. 11 also highlights the need to couple the model to some representation of stratocumulus. In particular, for large values of divergence, and a conditionally stable atmosphere, one would not expect mass fluxes to be effective in venting a subcloud layer. Rather condensate should accumulate at the top of the PBL, promoting increased cloud-top radiative cooling leading to entrainment deepening of the PBL possibly accompanied by a lowering of the LCL, and hence the development of a stratiform cloud layer. Mathematically this amounts to identifying mechanisms for limiting the convective venting of the layer as controlled by a_c. These issues and some proposals for doing so are discussed by [37]; in implementing them in the current framework one would look for the behavior of the solutions over the eastern boundary regions of the subtropical oceans, where surface fluxes are too low, and the cloud layer too shallow, to improve.

The model equilibrium can be solved for as an implicit system of algebraic equations using standard iterative techniques. Skipping the storage terms in the prognostic Eqs. (1), (5), and (6) gives a set of simultaneous equations. The solution of this system (not shown) corresponds exactly to the final equilibrium state that is reached in the time-dependent model.

In bulk models the mass flux does not appear in the prognostic budget equations for humidity and temperature. However, in multilayer discretized models, such as single-column models used in numerical weather prediction and climate models, mixed-layer height h can fall in between gridpoints. As the associated tendencies reflect the changing boundary-layer height, the mass flux then appears in the $\{q_t, \theta_l\}$ budget equations. This does not change the nature of the feedback mechanisms as present in the current model. A boosted mass flux would quickly decrease humidity in the layer below, in effect lowering mixed-layer height.
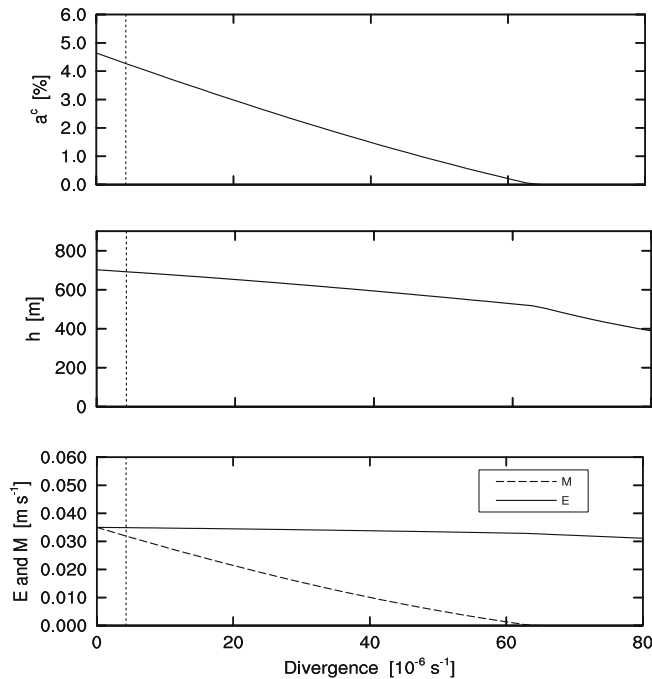

Fig. 11 Sensitivity test for large-scale divergence D in BOMEX case. **a** Convective area-fraction a^c. **b** Mixed-layer top h. **c** Entrainment E and mass flux M. *Dotted line*: value of D in standard BOMEX case

6 Conclusions

A simple bulk model is formulated for the shallow-cumulus-topped mixed layer. The essential novelty in the approach is that the convective area-fraction is retained in the mass-flux closure. This fraction now depends on the state of the system, being a function of humidity and variance at the mixed-layer top. This represents an extra degree of freedom in the convective mass flux and introduces a strong negative feedback in the system of equations. We call this mechanism the mass-flux humidity feedback. It is shown here to help determine the character of the equilibrium such that the mixed-layer top is always maintained close to cloud base. This condition was used as a constraint in previous equilibrium models [1,8].

The model reproduces the basic characteristics of the convective area-fraction and mass flux, boundary-layer structure, turbulent thermodynamic variances, and surface latent and sensible heat fluxes, as observed in nature, LES, and ERA40. The cloud state and the surface fluxes are difficult aspects of convective boundary layers to reproduce and therefore are a good indicator of model performance. The stability of the equilibrium state is corroborated by the observed persistent presence of shallow cumulus in the trade-wind regions.

These results show that the climatology of shallow-cumulus-capped boundary layers in the trades can be explained by the subcloud mixed-layer budgets. Such tight coupling of moist convection to subcloud-layer or surface-layer properties has been used in other recent modeling efforts [6,13]. In addition to bulk mixed-layer properties, the characteristics of the transition layer at cumulus cloud bases are taken into account through the local saturation deficit and turbulent variance that appear in the statistical closure for the convective area-fraction. The bulk subcloud-layer properties that determine the saturation characteristics of the transition layer, and thus the area fraction of shallow cumulus, act as a regulator or valve on the moist convective transport. This is due to the strong sensitivity of the mass flux to the cloud fraction, as illustrated by the perturbation analysis for the BOMEX case. The robustness of the system is quantified by the associated modest perturbation in mixed-layer depth.

The simple formulation of the mass-flux model makes it potentially useful for climate modeling purposes. The associated long integration times require simple but accurate parameterizations of subgrid processes. The interactive climate run of the QTCM model featuring this mass-flux model shows that on climatological time scales the extra degree of freedom in the mass flux closure always acts to keep the boundary layer close to the natural equilibrium state. In climate predictions cloud representation remains one of the most significant sources of uncertainty, and accordingly the representativeness of the equilibrium state of cloudiness as implied by parameterizations should receive much attention. We hope that this model can provide more insight into this problem.

References

1. Albrecht, B.A., Betts, A.K., Schubert, W.H., Cox, S.K.: A model of the thermodynamic structure of the Trade-wind boundary layer. Part I: Theoretical formulation and sensitivity tests. J. Atmos. Sci. **36**, 73–89 (1979)
2. Albrecht, B.A., Bretherton, C.S., Johnson, D., Schubert, W.H., Frisch, A.S.: The Atlantic stratocumulus transition experiment—ASTEX. Bull. Am. Meteorol. Soc. **76**, 889–904 (1995)
3. Anthes, R.A., Keyser, D.: Tests of a fine-mesh model over Europe and the United States. Mon. Wea. Rev. **107**, 963–984 (1979)
4. Augstein, E., Riehl, H., Ostapoff, F., Wagner, V.: Mass and energy transports in an undisturbed Atlantic trade-wind flow. Mon. Wea. Rev. **101**, 101–111 (1973)
5. Augstein, E., Schmidt, H., Wagner, V.: The vertical structure of the atmospheric planetary boundary layer in undisturbed Trade winds over the Atlantic Ocean. Bound. Layer Meteorol. **6**, 129–150 (1974)
6. Berg, L.K., Stull, R.B.: Parameterization of joint frequency distributions of potential temperature and water vapor mixing ratio in the daytime convective boundary layer. J. Atmos. Sci. **61**, 813–828 (2004)
7. Betts, A.K.: Non-precipitating cumulus convection and its parameterization. Q. J. R. Meteorol. Soc. **99**, 178–196 (1973)
8. Betts, A.K.: Modeling subcloud layer structure and interaction with a shallow cumulus layer. J. Atmos. Sci. **33**, 2363–2382 (1976)
9. Betts, A.K., Ridgway, W.: Climatic equilibrium of the atmospheric convective boundary layer over the tropical ocean. J. Atmos. Sci. **46**, 2621–2641 (1989)
10. Bretherton, C.S., Wyant, M.C.: Moisture transport, lower-tropospheric stability, and decoupling of cloud-topped boundary layers. J. Atmos. Sci. **54**, 148–167 (1997)

11. Bretherton, C.S., McCaa, J.R., Grenier, H.: A new parameterization for shallow cumulus convection and its application to marine subtropical cloud-topped boundary layers. Part I: description and 1D results. Mon. Wea. Rev. **132**, 864–882 (2004)
12. Brown, A.R., Chlond, A., Golaz, C., Khairoutdinov, M., Lewellen, D.C., Lock, A.P., MacVean, M.K. Moeng, C-H., Neggers, R.A.J., Siebesma, A.P., Stevens, B.: Large-eddy simulation of the diurnal cycle of shallow cumulus convection over land. Q. J. R. Meteorol. Soc. **128**, 1075–1094 (2002)
13. Cheinet, S. : A multiple mass flux parameterization for the surface-generated convection. Part II: Cloudy cores. J. Atmos. Sci. **61**, 1093–1113 (2004)
14. Cuijpers, H., Duynkerke, P.G.: Large-eddy simulation of trade-wind cumulus clouds. J. Atmos. Sci. **50**, 3894–3908 (1993)
15. Cuijpers, H., Bechtold, P.: A simple parameterization of cloud water related variables for use in boundary layer models. J. Atmos. Sci. **52**, 2486–2490 (1995)
16. Deardorff, J.W.: Convective velocity and temperature scales for the unstable planetary boundary layer and for Rayleigh convection. J. Atmos. Sci. **27**, 1211–1212 (1970)
17. Garratt, J.R.: Review of drag coefficients over oceans and continents. Mon. Wea. Rev. **105**, 915–929 (1977)
18. Grant, A.L.M.: Cloud-base fluxes in the cumulus-capped boundary layer. Q. J. Roy. Meteorol. Soc. **127**, 407–422 (2001)
19. Grant, A.L.M., Brown, A.R.: A similarity hypothesis for shallow-cumulus transports. Q. J. R. Meteorol. Soc. **125**, 1913–1936 (1999)
20. Holland, J.Z., Rasmusson, E.M.: Measurement of atmospheric mass, energy and momentum budgets over a 500-kilometer square of tropical ocean. Mon. Wea. Rev. **101**, 44–55 (1973)
21. Lenderink, G., Siebesma, P., Cheinet, S., Irons, S., Jones, C.G., Marquet, P., Müller, F., Olmeda, D., Calvo, J., Sanchez, E., Soares, P.M.M.: The diurnal cycle of shallow cumulus clouds over land: a single column model intercomparison study. Q. J. R. Meteorol. Soc. **130**, 3339–3364 (2004)
22. Lilly, D.K.: Models of cloud-topped mixed layers under a strong inversion. Q. J. R. Meteorol. Soc. **84**, 292–309 (1968)
23. Neelin, J.D., Zeng, N.: A quasi-equilibrium tropical circulation model–formulation. J. Atmos. Sci. **57**, 1741–1766 (2000)
24. Neggers, R.A.J., Siebesma, A.P., Lenderink, G., Holtslag, A.A.M.: An evaluation of mass flux closures for diurnal cycles of shallow cumulus. Mon. Wea. Rev. **132**, 2525–2538 (2004)
25. Neggers, R.A.J., Stevens, B., Neelin, J.D.: Variance scaling in shallow cumulus topped mixed layers. Q. J. R. Meteorol. Soc. August 2006 (submitted)
26. Neggers, R.A.J., Neelin, J.D., Stevens, B.: Impact mechanisms of shallow cumulus convection on tropical climate dynamics. J. Clim. July 2006 (accepted pending minor revisions)
27. Nicholls, S., LeMone, M.A.: The fair weather boundary layer in GATE: the relationship of subcloud fluxes and structure to the distribution and enhancement of cumulus clouds. J. Atmos. Sci. **37**, 2051–2067 (1980)
28. Nitta, T., Esbensen, S.: Heat and moisture budget analyses using BOMEX data. Mon. Wea. Rev. **102**, 17–28 (1974)
29. Norris, J.R.: Low cloud type over the ocean from surface observations. Part II: geographical and seasonal variations. J. Clim. **11**, 383–403 (1998)
30. Ooyama, K.: A theory on parameterization of cumulus convection. J. Meteorol. Soc. Jpn. **49**, 744–756 (1971)
31. Riehl, H., Yeh, C., Malkus, J.S., LaSeur, N.E.: The northeast trade of the Pacific Ocean. Q. J. R. Meteor. Soc. **77**, 598–626 (1951)
32. Schubert, W.H.: Experiments with Lilly's cloud-topped mixed layer model. J. Atmos. Sci. **33**, 436–446 (1976)
33. Siebesma, A.P., Cuijpers : Evaluation of parametric assumptions for shallow cumulus convection. J. Atmos. Sci. **52**, 650–666 (1995)
34. Siebesma, A.P., Bretherton, C.S., Brown, A., Chlond, A., Cuxart, J., Duynkerke, P.G., Jiang, H., Khairoutdinov, M., Lewellen, D., Moeng, C.-H., Sanchez, E., Stevens, B., Stevens, D.E.: A large eddy simulation intercomparison study of shallow cumulus convection. J. Atmos. Sci. **60**, 1201–1219 (2003)
35. Siebesma, A.P., Jakob, C., Lenderink, G., Neggers, R.A.J., Teixeira, J., Van Meijgaard, E., Calvo, J., Chlond, A., Grenier, H., Jones, C., Koehler, M., Kitagawa, H., Marquet, P., Lock, A.P., Muller, F., Olmeda, D., Severijns, C.: Cloud representation in general-circulation models over the northern Pacific Ocean: a EUROCS intercomparison study. Q. J. Meteorol. Soc. **130**, 1–23 (2004)
36. Sommeria, G., Deardorff, J.W.: Subgrid-scale condensation in models of non-precipitating clouds. J. Atmos. Sci. **34**, 344–355 (1977)
37. Stevens, B.: Boundary layer concepts for simplified models of tropical dynamics. Theor. Comput. Fluid Dyn. (in press) (2006)
38. Stevens, B., Ackerman, A.S., Albrecht, B.A., Brown, A.R., Chlond, A., Cuxart, J., Duynkerke, P.G., Lewellen, D.C., MacVean, M.K., Neggers, R.A.J., Sanchez, E., Siebsema, A.P., Stevens, D.E.: Simulations of Trade-wind cumuli under a strong inversion. J. Atmos. Sci. **58**, 1870–1891 (2001)
39. Stull, R.B.: An introduction to boundary layer meteorology. Kluwer, Dordrecht, p 670 (1988)
40. Yanai, M., Esbensen, S., Cho, J.H.: Determination of bulk properties of tropical cloud clusters from large-scale heat and moisture budgets. J. Atmos. Sci. **30**, 611–627 (1973)
41. Yin, B., Albrecht, B.A.: Spatial variability of atmospheric boundary layer structure over the eastern equatorial Pacific. J. Clim. **13**, 1574–1592 (2000)